Original Research

Laser Ablation Synthesis of Tin Oxide Nanoparticles and Their Thin-Film Properties

Liqaa S Ali [1,*]

[1] Ministry of Education, General Directorate of Education Baghdad, Karkh II, Baghdad 10001, Iraq
* Correspondence: liqaasadiq20@gmail.com

Received: December 4, 2025; Accepted: January 26, 2026

Abstract: Nanoparticles of tin oxide were hydrothermal synthesized by laser ablation in liquid using a Q-switched Nd:YAG laser at 1064 nm with energies ranging between 500 and 1000 mJ and temperature of 34 °C. The colloidal solutions obtained were drop mounted onto cleaned glass substrates to form thin films reaching ca. 200 nm thicknesses. The prepared films have been systematically studied with structural, morphological and optical features. The X-ray diffraction (XRD) characterization revealed the formation of polycrystalline tin oxide with a tetragonal crystal phase which mainly corresponds to the thermodynamically soluble SnO_2. A size of crystallite has been estimated by using Scherrer equation showing the dependence on laser energy. AFM analysis indicated that surface roughness and grain size decreased with increasing laser energy, which contributed to better surface uniformity. UV–Vis spectroscopy showed both improved optical absorption and a decrease of the optical band gap with increasing laser energy, attributed to defect induced localized states as well as band tailing effects rather than due to increased ordering. These findings underline the strong influence of the laser power on the structural and optical characteristics of tin oxide thin films for optoelectronic devices.

Keywords: SnO thin films; laser; nanoparticles; drop casting; AFM

1. Introduction

Tin oxide–based nanomaterials, including tin(II) oxide (SnO) and tin(IV) oxide (SnO_2), have attracted considerable attention owing to their unique optical, electronic, and catalytic properties[1]. These materials are widely utilized in various technological applications such as gas sensors, transparent conductive electrodes, photovoltaics, photocatalysts, and optoelectronic devices [2]. Among these, SnO_2 is the thermodynamically stable phase at ambient environment with wide band gap, high chemical stability and good optical transparent properties which are very desired for sensing and energy applications. Meanwhile, SnO is a nonstable phase, which can be obtained by certain preparation method and is attractive for its p-type semiconductor property. Tin oxide nanomaterials can be prepared via a number of physical and chemical methods such as sol-gel method, chemical vapor deposition (CVD), spray pyrolysis and thermal evaporation. But majority of such methods involved intricate processes, high reaction temperatures or chemical additives that bring the nanomaterials into risk of impurity contamination and lose their intrinsic nature. During the past few years, in this scenario, LAL has been shown to be a powerful physical method for the production of high-purity metal oxide NP if compared with chemical methods, in using as well as chemical precursors and surfactants [3]. In this context, laser ablation in liquid has emerged as an efficient physical technique for producing high-purity metal oxide nanoparticles without the use of chemical precursors or surfactants. In this method, a high-energy laser beam is focused onto a solid tin-based target immersed in a liquid medium, leading to material ejection, plasma formation, and subsequent nanoparticle generation [4], Laser ablation offers precise control over nanoparticle characteristics such as size, crystallinity, and defect concentration by tuning laser parameters,

particularly the laser energy [5]. Moreover, the absence of chemical reagents simplifies post-synthesis purification and preserves the intrinsic properties of the produced nanoparticles [6], A potential step to extend their use in functional devices is also the fabrication of thin films of these nanoparticles. Drop casting is an easy, low cost and available technique for preparing tin oxide thin films on glass substrates among different deposition methods [7]. The originality of the present work lies in the systematic investigation of the effect of laser energy on the structural, morphological, and optical properties of tin oxide nanoparticles synthesized by laser ablation in liquid and their corresponding thin films prepared by drop casting [8]. This study provides insight into phase stability, defect-related phenomena, and laser–matter interaction mechanisms, which are crucial for optimizing tin oxide thin films for optoelectronic and sensing applications.

2. Experimental

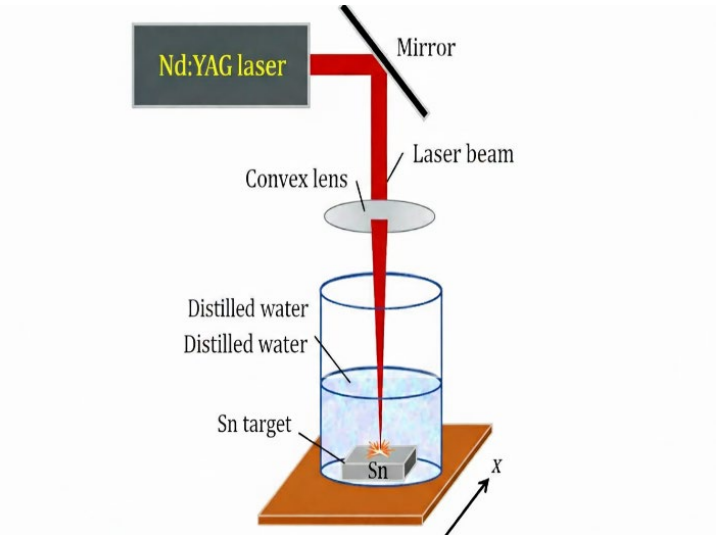

Figure 1. Schematic illustration of the laser ablation in liquid setup used for the synthesis of tin oxide nanoparticles.

Tin oxide nanoparticles were prepared by laser ablation in liquid (LAL) method, using a tin oxide target and deionized water at room temperature (34 °C). We used a Q-switched Nd:YAG laser at = 1064 nm as the ablation source. The laser is focused ~1 mm onto a stainless-steel tin oxide target at the base of a 30 ml glass cell containing deionised water. The distance between the focusing lens and the sample surface was ~20 cm. Ablation was performed for a time frame between 15 and 180 min, depending on the experiments [9]. Three laser energies, 500, 750 and 1000 mJ were selected to study the influence of the laser energy on nanoparticle formation. The HOLS and the target material interacted during the ablating process, and a plume form plasma was irradiated as a result to lead to fast ejection of matter and generation of tin oxide nanoparticles that were distributed in the liquid medium. The resulting colloidal solutions were a stable milky-white colour, which suggests that the nanoparticle syntheses were successful and keep the nanoparticle in suspension for long time periods [10]. The as-prepared colloidal solutions were drop-casted onto cleaned glass substrates of size 2 × 2 cm^2, to produce thin films. A pipette was used to transfer a fixed volume of the solution and 3 drops were uniformly dripped on each substrate. The thin films were then dried under 80 °C on hot plate to remove the residual solvent, then uniform thin film (thickness ~200 nm) was formed. The synthesized films were characterized structurally, morphologically and optically to investigate the role of laser energy on the film properties. A schematic diagram of the laser ablation system is shown in Figure 1.

3. Results and Discussion

3.1. Structural Properties

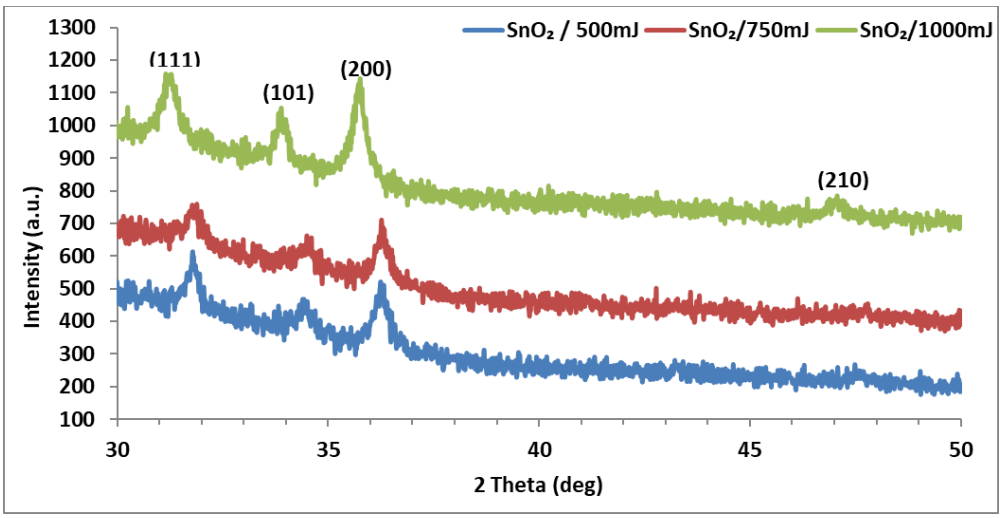

Figure 2. XRD patterns of all synthesized SnO thin films.

Figure 2 shows the X-ray diffraction (XRD) patterns of drop-casted tin oxide thin films at various laser fluences (500, 750 and 1000 mJ). All of the samples show sharp diffraction peaks, indicating that the deposited films are polycrystalline. The observed peaks with 2θ values of 33°, 35° and ~37° can be indexed to a tetragonal rutile structure of t-SnO_2 being the thermodynamically stable phase of tin oxide at ambient temperature. The lack of diffraction peaks for metallic tin suggests there is no free Sn within the detection limit of this XRD method. Nevertheless due to the metastable character of SnO, these films are more correctly termed as non-stoichiometric tin oxide (SnO_x), especially for low laser energy samples. A highly dependence of crystalline fraction on the laser energy is noticed. The 500 mJ film shown broad and the least intense diffraction peaks, as evidence of small crystallite size coupled with lattice strain and structural disorder. While the laser energy of 750 mJ is applied, diffraction peaks are sharpened and strengthened with improved crystallinity caused by growing well-crystal. Among the samples produced at 1000 mJ, the one exhibits narrow peak widths and high peak-intensity of maximum intensity shows better crystallinity with less microstrain. The calculated crystallite sizes according to Scherrer equation are listed in Table 1, and obviously show a change with laser energy and crystallographic orientation. Generally, value of FWHM for some diffracting planes increases (decrease in crystallite size) with an increase in laser power. This is assigned to the higher kinetic energy of ablated species at high laser energies that results in a greater defect formation, oxygen vacancy concentration and lattice distortion. Direction-dependent crystal growth is a characteristic of laser-ablated metal oxide thin films, and this anisotropic trend in crystallite size among different (hkl) planes is observed for the entire VRHPLG sample. Moreover, weak diffraction peak position changes are noticed when increasing the laser energy. These shifts are associated with lattice parameter variations induced by oxygen vacancies, non-stoichiometry effects, and residual stress within the films. Such structural distortions play a critical role in determining the optical behavior of the films, particularly the observed band gap narrowing discussed in subsequent sections [11, 12]. The crystallite size (D) was estimated using the Scherrer equation:

$$D = (K \times \lambda) / (\beta \times \cos\theta) \quad (1)$$

where:
- D is the crystallite size;
- K is the shape factor (0.9);
- λ is the X-ray wavelength (Cu Kα = 1.5406 Å);
- β is the full width at half maximum (FWHM) in radians;
- θ is the Bragg angle.

Table 1. Structural parameters of the fabricated films, determined at a uniform thickness of 200 nm.

Samples	2 Theta (deg)	β (deg)	D_g (nm)	(hkl)
SnO_2 (500 mJ)	31.67	1.0014	9.57	(111)
	34.39	0.227	42.63	(101)
	36.21	0.3954	24.41	(200)
SnO_2 (750 mJ)	31.58	1.5908	6.05	(111)
	34.49	0.3257	29.65	(101)
	36.24	0.3593	26.80	(200)
SnO_2 (1000 mJ)	31.09	1.6773	4.83	(111)
	33.88	0.273	29.46	(101)
	35.70	0.4205	19.05	(200)

Figure 3 shows the three-dimensional AFM images of tin oxide thin films deposited at three representative laser energies (500, 750 and 1000 mJ). AFM measurements demonstrate a pronounced dependence of surface morphology and roughness on the laser energy. On the film ablated at 500 mJ, a rough surface is presented with granular and non-uniform texture. The distribution of the grain is not uniform, and a large variation in height can be seen on the surface, suggesting relatively low surface-diffusion velocity by ablated species during film formation. The relatively large RMS roughness value is indicative of the existence of larger grains and structural disorder on the foils [13]. When laser traces are further increased up to 750 mJ, a significant enhancement in surface morphology can be observed. The film surface is smoother, and the grains distribution becomes even and compact than that of 500 mJ. Decreased RMS roughness indicated better surface diffusion and nucleation processes resulting in better homogenous films. At this intermediate laser energy particles kinetic energy and surface rearrangement is balanced, yielding a better quality surface for which the defects are not overwhelming. For the 1000 mJ deposited film the best surface features are obtained. The AFM image reveals a dense and flat surface containing uniformly dispersed fine grains with small height variation. With increasing MBN sol, the grain boundaries become harder to differentiate and the RMS roughness drops to its minimum value, reflecting a more uniform and dense surface. Decrease of grain size and roughness on increasing laser energy is due to more kinetic energy achieved in the ablated species, thus facilitating their surface diffusion and rearrangement during film growth. This tendency is also supported by calculated roughness parameters from AFM measurements, as shown in Table 2. The RMS roughness and the average surface roughness decrease systematically with increasing laser energy, together with a reduced grain size changing from its original large size to fine one. These results are consistent with the XRD analysis, where increased laser energy led to modified crystallite size and defect-induced lattice distortion. The improved surface uniformity at higher laser energies is particularly advantageous for optoelectronic and sensing applications, where smooth and compact thin films are essential [14].

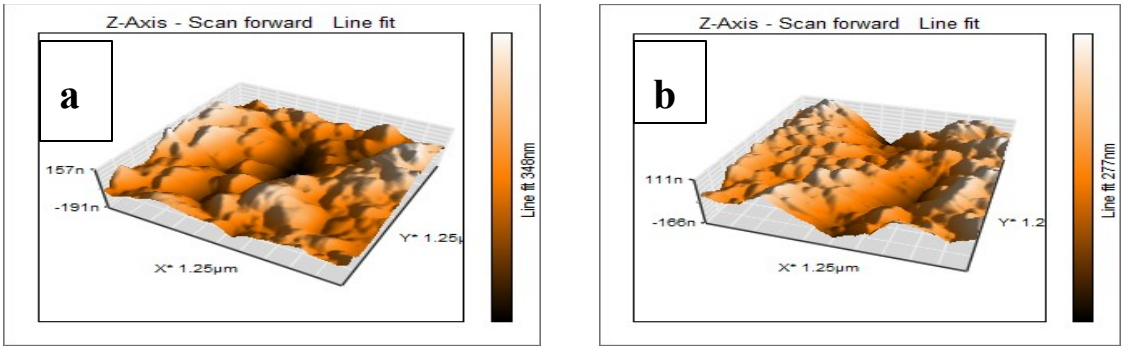

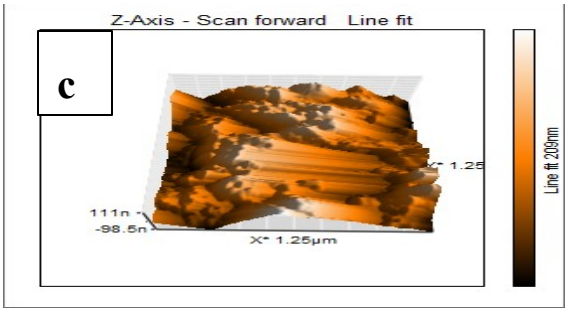

Figure 3. Three-dimensional AFM images of all deposited SnO thin films grown at laser energies of (a) 500, (b) 750, and (c) 1000 mJ.

Table 2. Surface roughness parameters of the films obtained from AFM analysis.

Sample	Size of grain (nm)	Roughness. (nm)	Root mean square. (nm)
SnO_2 (500 mJ)	Large	2.60	3.35
SnO_2 (750 mJ)	Medium	2.13	2.67
SnO_2 (1000 mJ)	Small	1.58	2.00

Figure 4 shows the FESEM surface micrographs of tin oxide thin films grown at various laser energies of 500, 750 and 1000 mJ. SEM observation reveals that the deposited films' surface texture and microstructure features are significantly influenced by laser energy. The surface of the film deposited at 500 mJ is rather rough and dense with ill defined grain boundaries. The lack of well defined grains points to a nanocrystalline structure with high degree of structural defects which can be related to low migration rate and reduced mobility the adatoms 35 at lower laser energy. This finding is in agreement with the wide diffraction peaks in XRD pattern and greater surface topography seen by AFM. When the pulse energy of the laser is 750 mJ, the good surface morphology is achieved. The movie is of medium granularity, characterized by partially grown grains and incipient grain boundaries. Such improvement is believed to be due to higher kinetic energy of the ablated species which allows achieving better atomic rearrangements and surface diffusion upon film growth. In consequence, improved crystal ordering and partial grain coalescence are realized. At the maximum laser energy of 1000 mJ, the SEM image shows uniform and clear granular structure. The surface is composed of grains finer in size and homogeneously dispersed with more defined boundaries, suggestive of increased microstructural ordering. The higher laser energy increases atom mobility and surface diffusion, facilitating efficient rearrangement and densification of the film. However, the formation of finer grains at higher energy is also associated with an increased density of defect-related nucleation sites, which is consistent with the reduced grain size observed in AFM measurements and the defect-induced effects inferred from XRD analysis. Overall, the SEM results corroborate the AFM and XRD findings, confirming that increasing laser energy leads to improved surface uniformity and microstructural organization of tin oxide thin films. These microstructural modifications play a significant role in governing the optical properties of the films discussed in the subsequent sections [15].

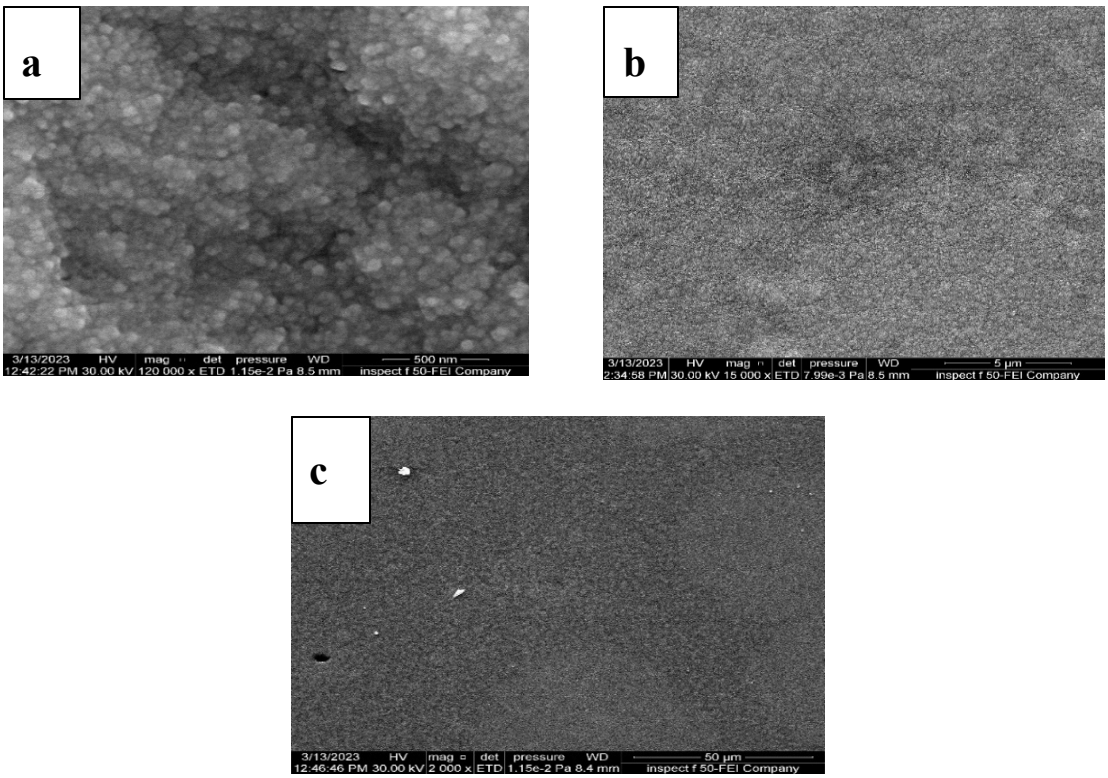

Figure 4. FESEM surface morphology images of synthesized SnO thin films grown at laser energies of (a) 500, (b) 750, and (c) 1000 mJ. Scale bar = 50 μm.

3.2. Optical Properties

Figure 5 displays the UV–Vis absorbance spectra of the SnO_2 thin films prepared at various laser energies (500, 750, and 1000 mJ) in the wavelength range of 350 to 1000 nm. All samples exhibit strong absorption in the UV region, which is typical for wide-band-gap semiconducting tin oxide materials. Highly absorption in UV region is due to the fundamental electronic transitions from valence band (VB) to conduction band (CB). It is clear that absorbance depends on laser energy. The 1000 mJ-prepared film has the most absorbance for the whole spectrum, followed by the 750 mJ- and 500 mJ-deposition films. Nevertheless, this enhanced absorbance at higher laser energies should not be directly associated to increased crystallinity / decreased defect density. This is also perhaps an indication of better crystallinity and lower grain boundary density which usually leads to lesser optical absorption in the visible spectral range. The increase of the absorbance at higher laser energies is mainly due to increased concentration in defect-related localized states like oxygen vacancies and Non-stoichiometry of SnOx phase. These defect states create extra energy levels in the band gap and result sub-bandgap absorption which ultimately leads to enhancement in light–matter interaction. Also, the grain structure becomes finer and surface area larger at higher laser energies; including large fractions of characteristic dimensions of plasmonic nanoparticles, which enhances the absorption by increased scattering and multiple internal reflections. These observations reveal that the laser power has a significant role in controlling the optical absorption behaviour of SnO_2 thin films. The higher-energy samples, particularly those prepared at 1000 mJ, exhibit enhanced optical absorption due to defect-mediated mechanisms, making them promising candidates for optoelectronic applications where strong light absorption is required, such as photodetectors and UV-sensitive devices [16].

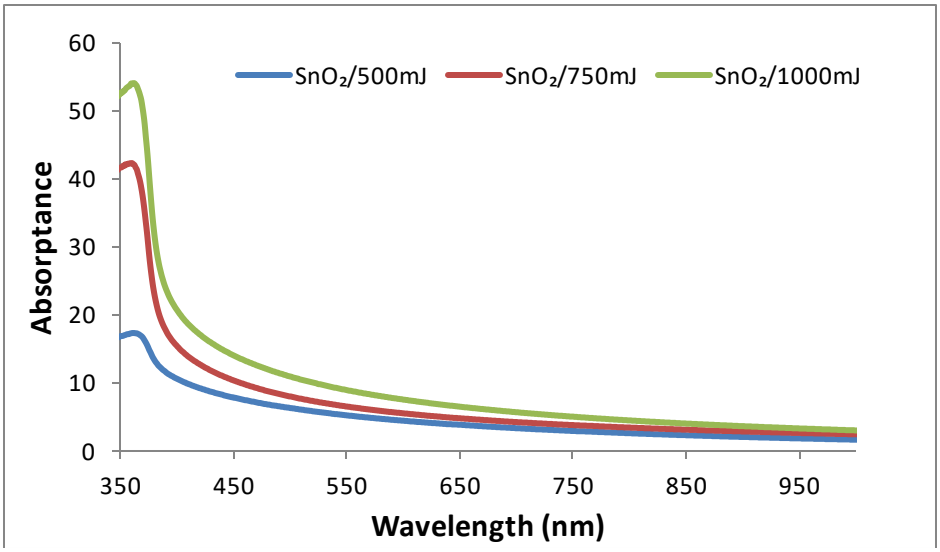

Figure 5. UV-Vis absorbance spectra of SnO thin films prepared at different laser energies (500 mJ, 750 mJ, and 1000 mJ), measured over the wavelength range of 350–1000 nm.

Figure 6 shows the change in the absorption coefficient (α) as a function of wavelength for SnO_2 thin film deposited at different laser energies (500, 750, and 1000 mJ). All the samples display high values of absorption coefficient in UV region, and show a tendency to decrease with increasing wavelength towards near infrared. This behavior is typical of wide bandgap semiconducting tin oxide materials and is due to basic electronic transitions in the vicinity of the absorption edge. An explicit relationship between the absorption coefficient and laser energy is demonstrated. The 1000 mJ coated film showed the highest α values over all measured wavelengths, followed by the 750 mJ sample and then by the 500 mJ one. Nevertheless, this increase in the absorption coefficient with increasing laser power should not be due to better crystallinity and fewer defect density. In contrast, denser, more crystalline etched films usually feature a decreased visible light absorption owing to diminished defect-related absorptive sites. A higher absorption coefficient at high laser energies can be mainly attributed to the defect-related local states, such as oxygen vacancies and non-stoichiometric SnO_x phases that produce more energy levels inside forbidden band. Such localized states can cause to elevate the level of sub-bandgap absorption and probability that a photon will be absorbed. Moreover, submicron grain sizes and the increase in surface roughness with increasing laser energy can enhance light scattering and multiple internal reflections which could result in higher effective absorption. The large increase in α for $\lambda < \sim 400$ nm is due to strong intrinsic absorption resulting from band-to-band electronic transitions. The high absorption coefficient values, particularly for the sample prepared at 1000 mJ, indicate that the films are capable of absorbing a significant fraction of incident UV radiation. This characteristic is advantageous for optoelectronic applications such as UV photodetectors and light-sensitive devices, where defect-assisted absorption mechanisms can play a beneficial role.

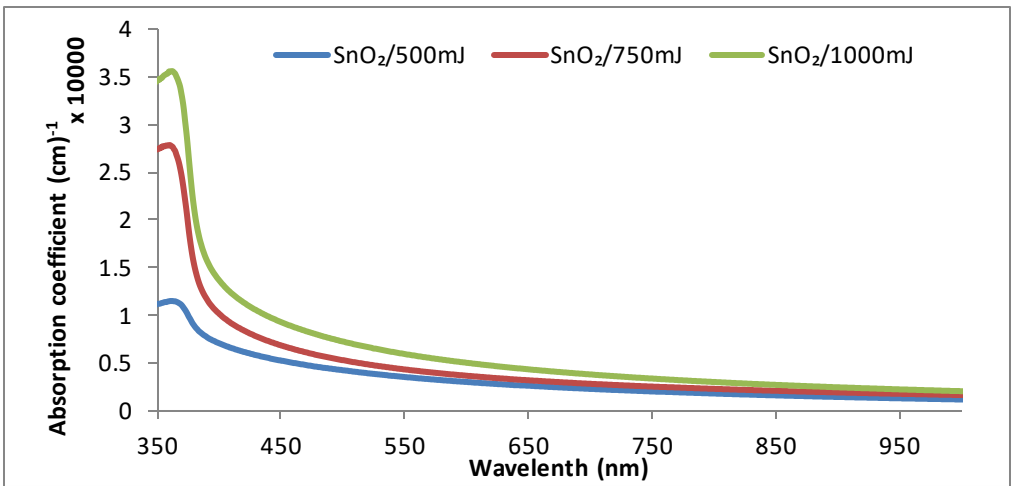

Figure 6. Variation of the absorption coefficient (α) with wavelength for SnO thin films deposited at laser energies of 500 mJ, 750 mJ, and 1000 mJ.

Figure 7 presents the Tauc plots used to determine the optical band gap energy (Eg) of tin oxide thin films deposited at different laser energies (500, 750, and 1000 mJ). The optical band gap values were estimated by extrapolating the linear portion of the $(\alpha h\nu)^2$ versus photon energy ($h\nu$) curves to the energy axis. The estimated Eg values are approximately 3.2 eV for the film prepared at 500 mJ, 2.8 eV for the 750 mJ sample, and 2.6 eV for the 1000 mJ sample. A systematic reduction in the optical band gap with increasing laser energy is clearly observed. However, this band gap narrowing should not be interpreted as a consequence of improved crystallinity or reduced defect density. Instead, the decrease in Eg is primarily attributed to the increased concentration of defect-related localized states, such as oxygen vacancies and non-stoichiometric SnO_x phases, which introduce tail states near the band edges. These localized states lead to band tailing effects and effectively reduce the optical band gap. In addition, variations in nanoparticle size and microstructural disorder may also contribute to the observed band gap narrowing. Although quantum confinement effects are typically expected to increase the band gap for very small particle sizes, the particle dimensions in the present study suggest that defect-induced band tailing is the dominant mechanism governing the observed optical behavior [12]. The correlation between reduced crystallite size, increased defect density, and band gap narrowing is consistent with the structural and morphological analyses obtained from XRD, AFM, and SEM measurements. These results demonstrate that laser energy is a critical parameter for controlling the defect structure and electronic band structure of tin oxide thin films, enabling tunability of their optical properties for optoelectronic applications.

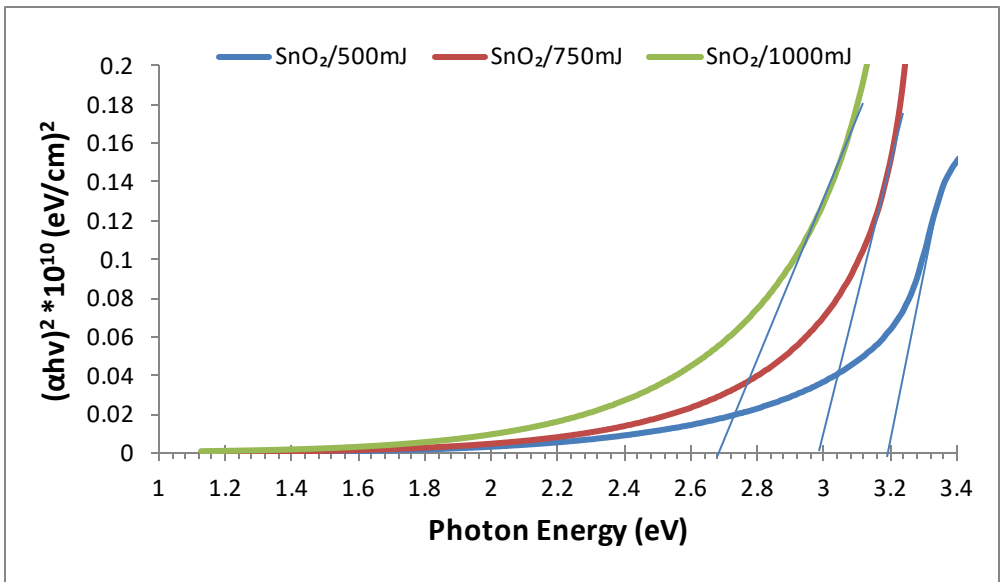

Figure 7. Tauc plots for determining the optical bandgap energy of SnO thin films deposited at laser energies of 500 mJ, 750 mJ, and 1000 mJ.

4. Conclusions

The tin oxide thin films were prepared by the laser ablation in liquid technique (LAL) combined with drop-casting deposition and its effect on their structural, morphological and optical properties was studied as a function of LAL energy. The structural study indicates that the laser energy is an important parameter in determining crystallite size, lattice strain, defect and disorder formation in the film. XRD data verified the polycrystalline character of the deposited films mostly consisting of non-stoichiometric tin oxide (SnO_x) with thermodynamically stable SnO_2 phase. The changes of peak shape and position observed with respect to the laser energy could be assigned not only to lattice distortion, oxygen vacancy but also non-stoichiomteric effects for that of a better crystalline structure. AFM and SEM observations revealed improved surface uniformity with higher laser energy. Increased laser energies yielded smoother surfaces, lower roughness and finer distribution of grain that could be related to increased surface diffusion and defect-assisted nucleation leading to the film growth. The film prepared at 1000 mJ showed the minimum surface roughness and a uniform morphology among the samples studied. Optical measurements showed improved absorption and a gradual decrease in the optical band gap as the laser energy was increased. This band gap narrowing was attributed to defect-induced localized states and band tailing effects arising from oxygen vacancies and non-stoichiometric phases, rather than improved structural order. The film prepared at 1000 mJ exhibited the highest optical absorption and the lowest band gap energy, indicating a strong influence of defect-related states on the optical behavior. Overall, the results demonstrate that laser energy is an effective parameter for tailoring the defect structure, surface morphology, and optical properties of tin oxide thin films. The films deposited at higher laser energies, particularly 1000 mJ, show promising characteristics for optoelectronic and sensing applications where enhanced absorption and defect-mediated electronic states are advantageous. Further advanced characterizations such as TEM, XPS, and PL spectroscopy are expected to provide deeper insight into the phase composition and defect-related mechanisms in future studies.

Acknowledgments: Not applicable.

Availability of Data and Materials: The data used and analyzed during the current study are available from the corresponding author upon reasonable request.

Funding: This research received no external funding.

Author Contributions: The single author had the sole role in designing, data collecting, analyzing, and writing the manuscript.

Conflicts of Interest: The author declares no conflict of interest.

References

1. Gürbüz, M. Nanosized Metaloxide Semiconductor Coating with Electrospraying Method for Sensor Application (Turkish) [Master's thesis]. Anadolu University; 2007.
2. Zaytsev, V.B.; Zhukova, A.A.; Rumyantseva, M.N.; et al. Antimony doped whiskers of SnO_2 grown from vapor phase. *Journal of Crystal Growth* 2010, 312(3), 386–390. https://doi.org/10.1016/j.jcrysgro.2009.11.022
3. Açıksarı, C. Production of High Purity Nanosized SnO_2 Powder Used as Target Material For Gas Sensor Applications (Turkish) [Master's thesis]. Anadolu University; 2014.
4. Khelifi, C. Tin Dioxide SnO_2 Thin Films Deposited by Ultrasonic Spray Technique: Properties and Applications [PhD thesis]. University of Med Khider Biskra; 2018.
5. Zhou, J.; Yang, H.; Xu, N.; et al. Enhanced effect of non-stoichiometry on the sinterability and microwave dielectric properties of $Mg_{2+x}SnO_4$ ceramics. *Journal of Materials Science: Materials in Electronics* 2014, 25, 500–504. https://doi.org/10.1007/s10854-013-1615-2
6. Hazem, A.; Mustafa, M.H. Influence of silver doping on the properties of sprayed cadmium telluride films. *Journal of Physics: Conference Series* 2025, 3028(1), 012048. https://doi.org/10.1088/1742-6596/3028/1/012048
7. Zhou, X.; Meng, Z.; She, J.; et al. Near-infrared light-responsive nitric oxide delivery platform for enhanced radioimmunotherapy. *Nano-Micro Letters* 2020, 12, 1–14. https://doi.org/10.1007/s40820-020-00431-3
8. Ali, L.S.; Shihab A.A. The effect of annealing temperature on Ag_2Te thin films' optical and structural characteristics. *AIP Conference Proceedings* 2025, 3211(1), 060006. https://doi.org/10.1063/5.0257111
9. Köse, H. Production of SnO_2/Mwcnt Nanocomposite Anode For Lithium Ion Batteries by Sol-Gel Method [PhD thesis] (Turkish). Sakarya Universitesi (Turkey); 2014.
10. Ali, L.S.; Shehab, A.A.; Abd, A.N. Influence of Li Doping in NiO thin films prepared by simple chemical method. *Journal of Global Pharma Technology* 2009, 224–230.
11. Rahaman, M.M.; Hussain, K.M.A.; Sharmin, M.; et al. Structure, morphology and opto-electrical properties of nanostructured indium doped SnO_2 thin films deposited by thermal evaporation. *European Scientific Journal ESJ* 2016, 12, 263–275. https://doi.org/10.19044/esj.2016.v12n27p263
12. Mohamed, S.H.; Khan, M.T.; Almohammedi, A.; et al. Synthesis, structural and photophysical properties of mixed Zn: SnO_2 nanowires. *Materials Science in Semiconductor Processing* 2021, 123, 105573. https://doi.org/10.1016/j.mssp.2020.105573
13. Karslıoğlu, R. Production of Sno_2 Coating by used Chamical Vapour Deposition(CVD) [Master's thesis] (Turkish). Sakarya Universitesi (Turkey); 2007.
14. Lin, Y.H. Structure and Properties of Transparent Conductive ZnO Films Grown by Pulsed Laser Deposition (PLD) [PhD thesis]. University of Birmingham; 2010.
15. Kurşungöz, C. Biological Applications of Nanoparticles Produced by Laser Ablation Method [PhD thesis]. Bilkent Universitesi (Turkey); 2017.
16. Pan, X.Q.; Fu, L. Tin oxide thin films grown on the (1012) sapphire substrate. *Journal of Electroceramics* 2001, 7, 35–46. https://doi.org/10.1023/A:1012270927642